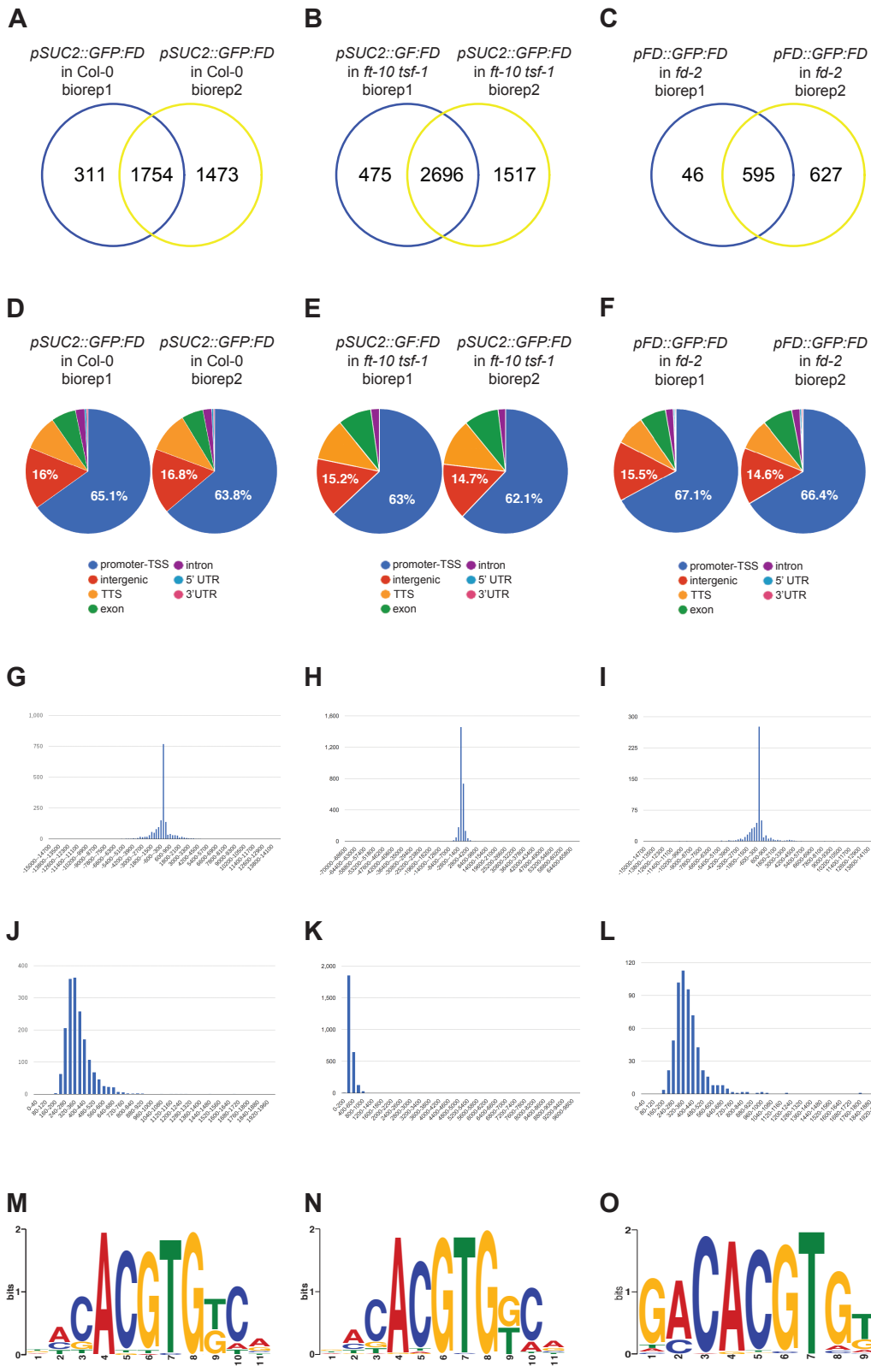

Figure S1. ChIP-seq summary statistics for the different biological replicates: *pSUC2::GFP:FD* in Col-0 (A, D, G, J, M) and *ft-10 tsf-1* mutant background (B, E, H, K, N), *pFD::GFP:FD* in *fd-2* mutant background (C, F, I, L, O).

(A-C) Annotation of high-confidence peaks found in different biological replicates.

(D-F) 2-set venn diagram showing the overlap of FD-bound peaks between two biological replicates.

(G-I) Distribution of the distance to the nearest TSS for the shared peaks.

(J-L) Distribution of the width of the peak for the shared peaks.

(M-O) Nucleotide logo of the predicted FD binding site based on peaks regions shared between biological replicates.

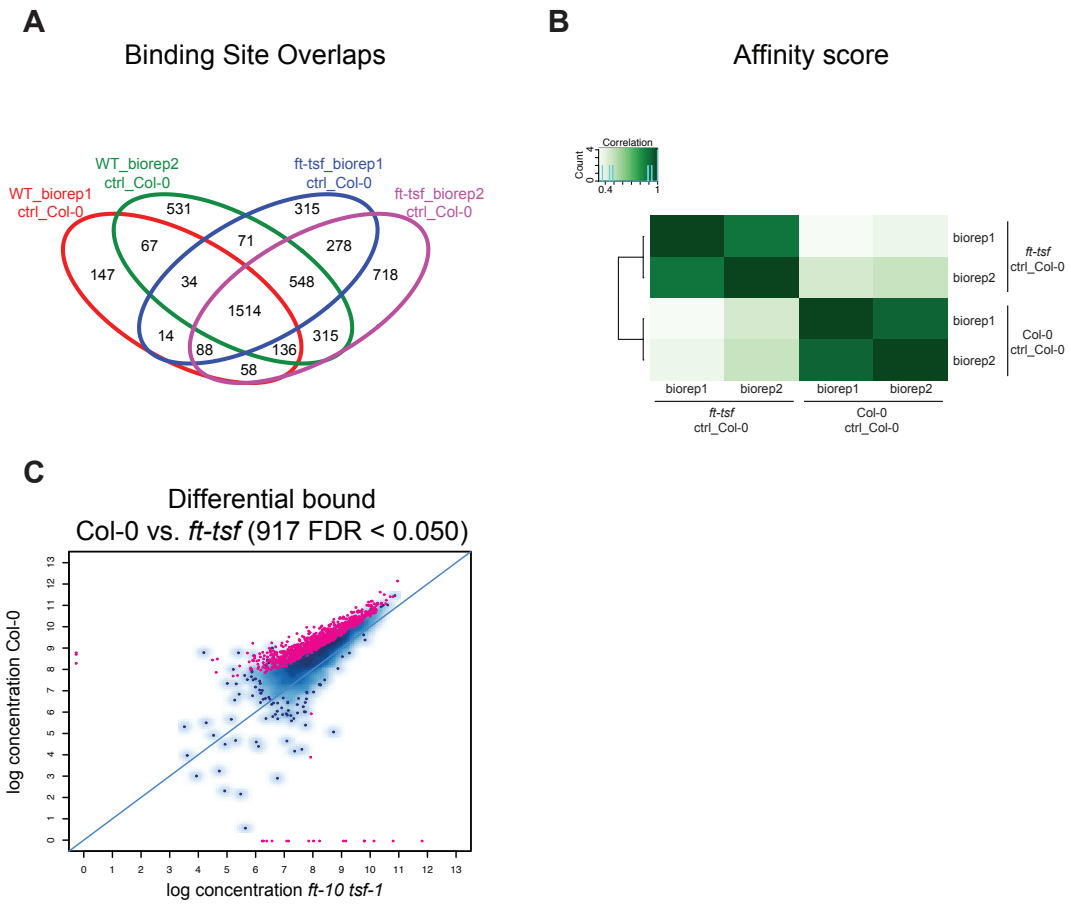

Figure S2. Verification of comparability of controls used for normalization of FD (*pSUC2::GFP:FD*) ChIP-seq in Col-0 and *ft-10 tsf-1* seedlings.

To test the robustness of results reported in Fig. 1B-E and to confirm that the usage of two different backgrounds as controls did not introduce any undue bias in peaks calling, we used *pSUC2::GFP:NLS* in Col-0 also for normalization of the experiments conducted in *ft-10 tsf-1*.

(A) 4-set venn diagram of the overlapping of the four biological replicates using only the controls in Col-0. Numbers are very similar to the ones reported in Fig. 1B.

(B) Correlation heatmap calculated on a binding matrix based on ChIP-seq reads counts for each samples (affinity scores) confirms that biological replicates still cluster by genotype.

(C) A total of 917 peaks were found as differentially bound (FDR < 0.05) between WT and *ft-10 tsf-1* using *pSUC2::GFP:NLS* in Col-0 as the unique control, which is very similar to 885 reported in Fig. 1E.

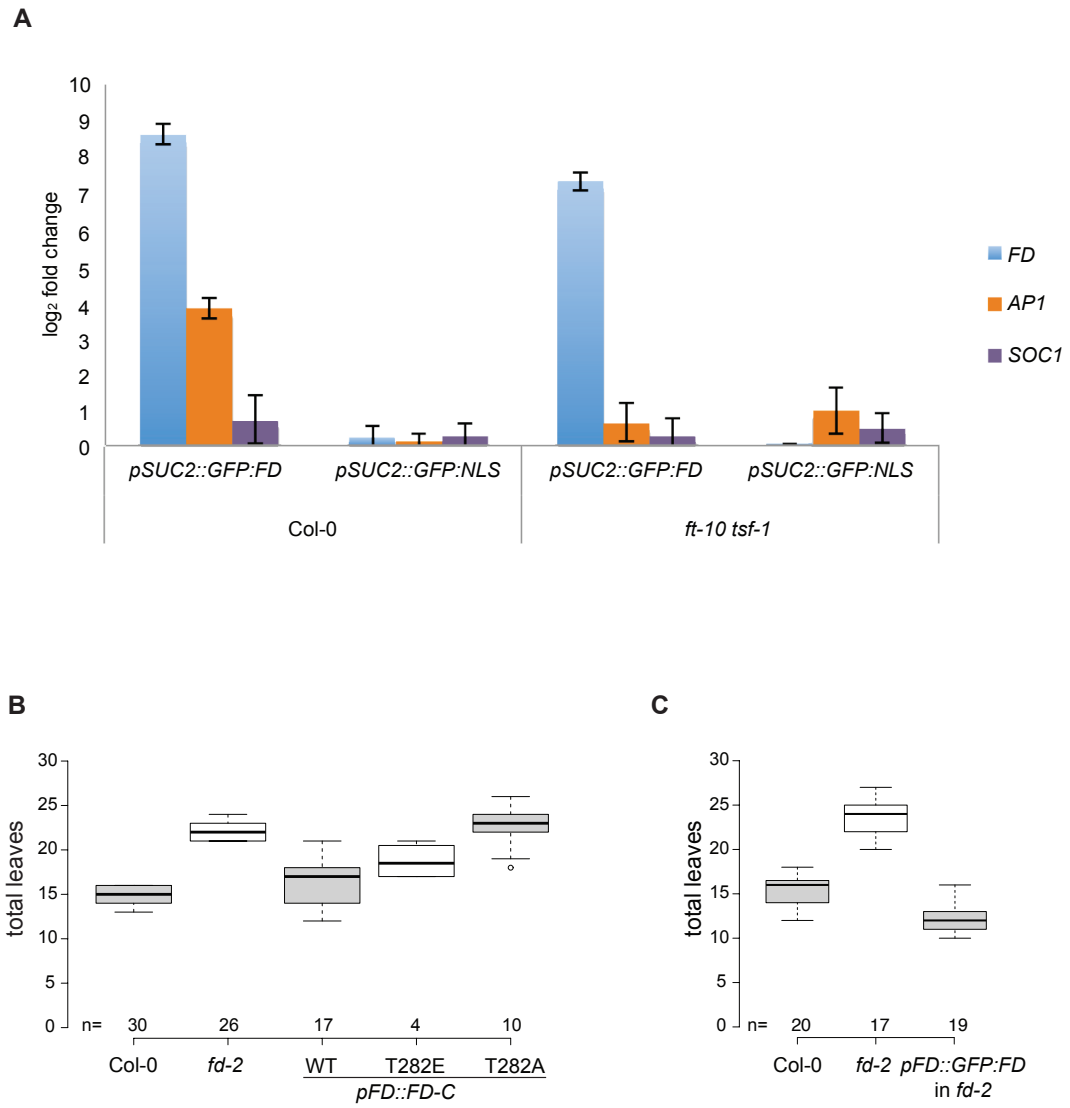

Figure S3. Effect of misexpression of FD on gene expression and flowering time.

(A) Expression analysis of *FD*, *AP1* and *SOC1* in *pSUC2::GFP:FD* and *pSUC2::GFP:NLS* in Col-0 and *ft-10 tsf-1* mutant. Leaves were collected from 16 days old seedlings carrying *pSUC2::GFP:FD* and *pSUC2::GFP:NLS* both in Col-0 and *ft-10 tsf-1* mutant grown under LD at 23ºC. *FD* is strongly induced in leaves only when expressed under SUC2 promoter. The strong induction of *FD* in leaves induce only the expression of *AP1,* but not of *SOC1*, in Col-0 compared to *ft-10 tsf-1* mutant.

(B) Flowering time of *fd-2* expressing the C-terminal fragment of FD under control of the pFD promoter. The unaltered version (WT), the phosphomic version (T282E), and the non-phosphorable version (T282A) of the C-terminal fragment of FD (amino acids 203 – 285) were transformed in to *fd-2* and flowering time was scored in T1 plants after Basta treatment. Col-0 and *fd-2* plants were used as controls. Number of independent T1 plants is indicated.

(C) Complementation of *fd-2* by *pFD::GFP:FD*. Flowering time of *fd-2* mutants transformed with *pFD::GFP:FD* to demonstrate the activity of GFP:FD fusion protein. Flowering time was scored as total leaves number (B). Col-0 and *fd-2* plants were used as controls. Number of plants is indicated.

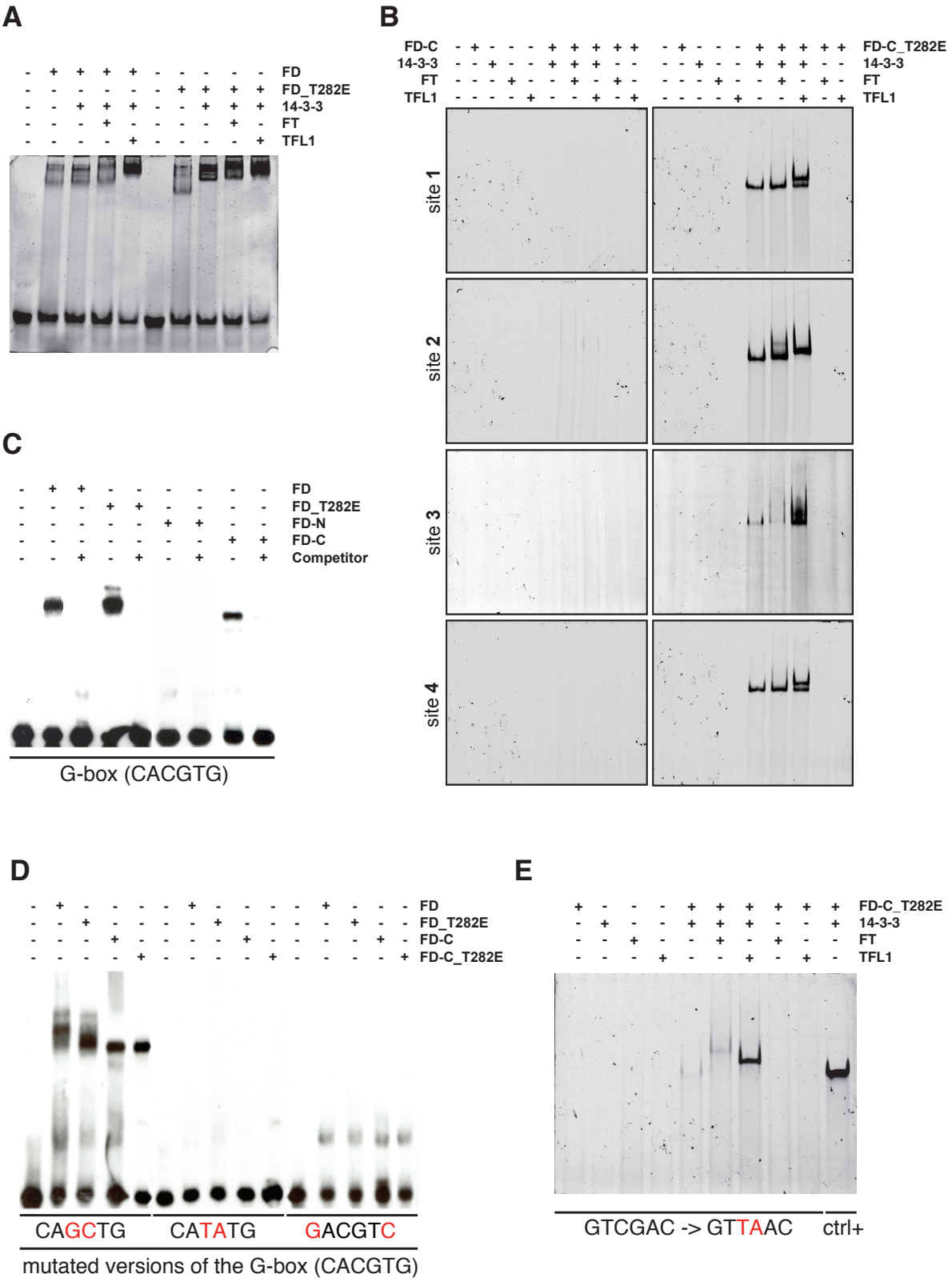

Figure S4. Electrophoretic mobility shift assays (EMSAs) to test FD binding to the *SEP3* and *AP1* promoters.

(A) Wildtype and phosphomic (T282E) versions of full-length FD protein bind the G-box from *SEP3* promoter in the absence of interaction partners. Higher order complexes are formed in the presence of 14-3-3v and FT or TFL1, essentially confirming results obtained using a C-terminal fragment of FD (amino acids 203 – 285; Fig. 2).

(B) Comparison of the wildtype and phosphomimic version of FD-C (FD-C_T282E) in combinations with 14-3-3v, FT and TFL1 using the four putative binding sites in the *AP1* promoter reported in Fig. 4B. Free probes are not visible because gels were running longer to maximize the distance between shifted probes. Only the phospho-mimic version of FD-C (FD-C_T282E) forms higher order complexes and binds DNA.

(C) EMSAs to verify whether the C-terminal of FD alone (FD-C), which contains the DNA-binding domain, is sufficient to bind DNA and whether the N-terminal can interact with DNA.

(D) EMSAs to test the influence of different mutations of the G-box in the interaction of FD with DNA.

(E) EMSA to test whether the mutation on the site 2 on AP1 promoter is sufficient to abolish the interaction of FD with DNA reported in Fig. 4B. In “ctrl+” the probe containing the G-box from SEP3 was used.

EMSA reported in panels C and D were preliminar experiments in order to set the assay and were done with Chemiluminescent EMSA kit (ThermoFisher Scientific cat. 20148) according to the manufacters instructions. We then shifted to fluorescent labeled probes (see methods in the main text) because it is a faster, cheaper and more accurate method. Images reported in these panels come from different gels and were merged together for a better representation.

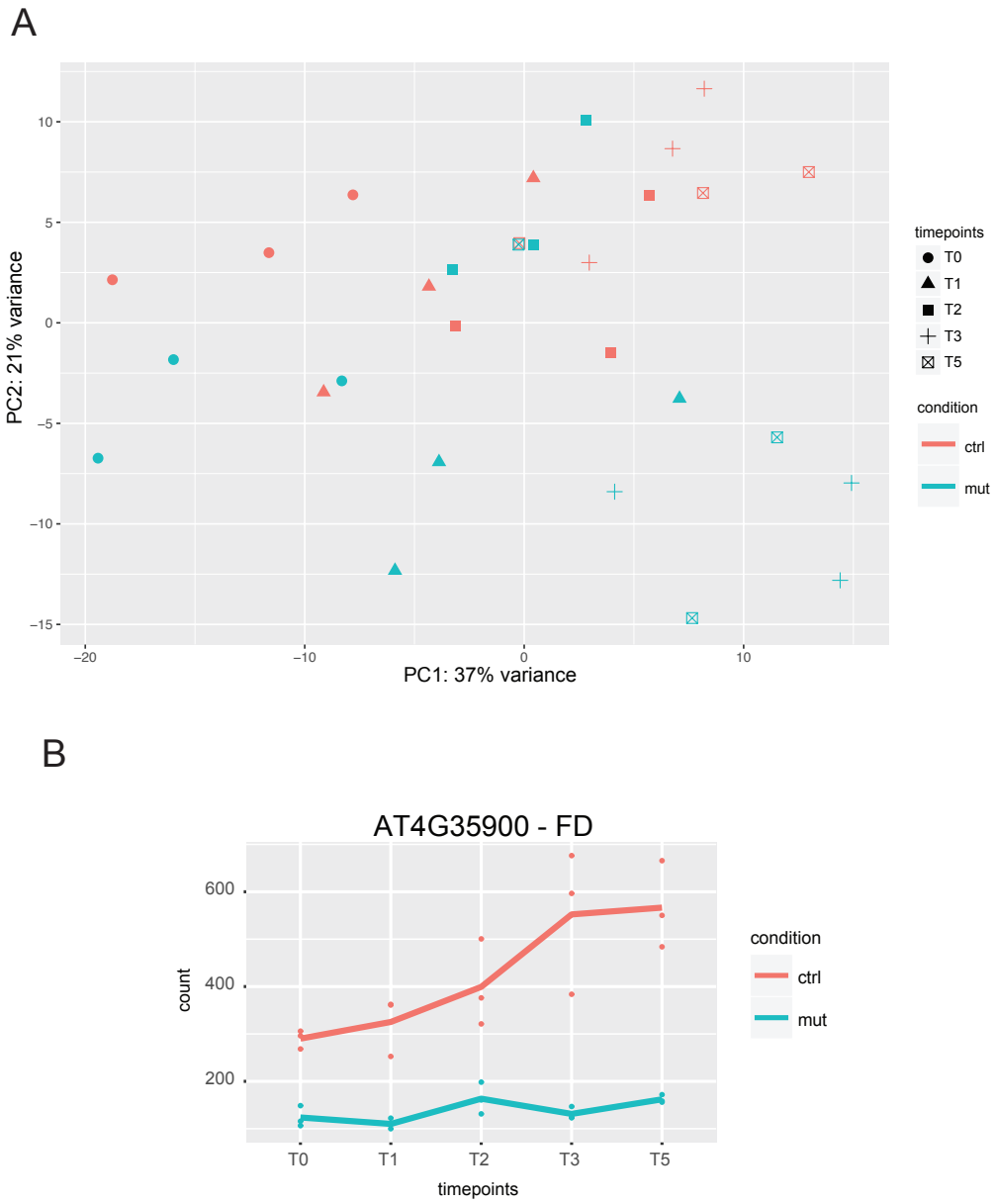

Figure S5. Summary of RNA-seq results.

(A) PCA analysis of 30 RNA-seq samples. 37% of the variance in the data set is explained by the different time points and 21% by the genotypes. Genotypes become visibly separated in time points T3 and T5. Red marks control samples (ctrl.; *pFD::GFP:FD fd-2*) and blue is used for *fd-2* mutant.

(B) Expression profile of FD in control and *fd-2* mutants. The expression of FD increases after T2 in agreement with the results showed in (A). Red dots indicate gene expression in control samples (*pFD::GFP:FD fd-2*), blue dots indicate gene expression in *fd-2*. Mean expression in control and *fd-2* is indicated by red and blue lines, respectively.

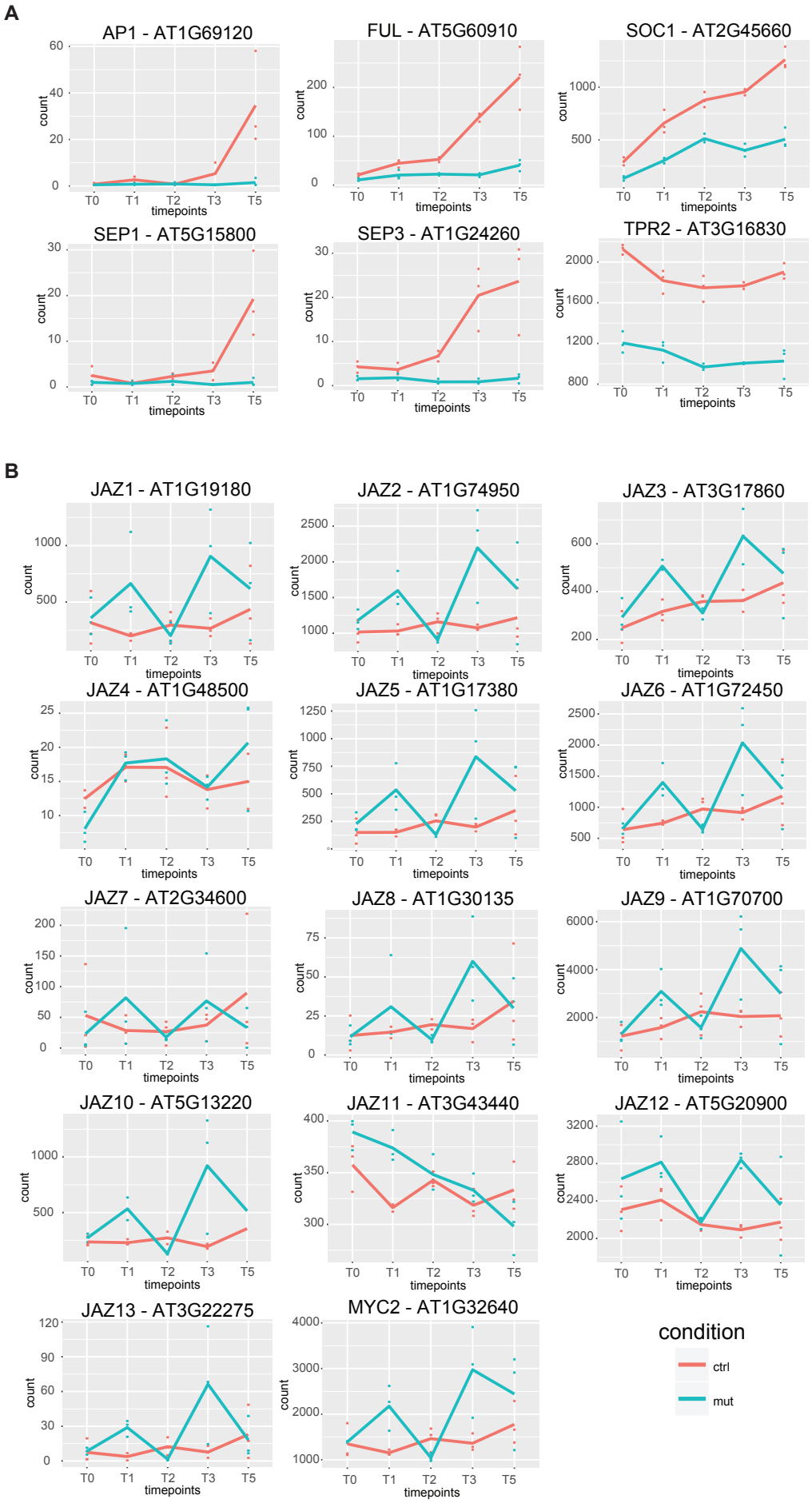

Figure S6. Expression profile of selected FD target genes.
(A) Expression profiles of *FD*, *AP1*, *FUL*, *SOC1*, *SEP3*, *SEP1*, and *TPR2* are reported.
(B) Expression profiles of 13 *JAZ* genes and *MYC2* at the shoot apical meristem for five time points during floral transition are shown.
Red dots indicate gene expression in control samples (*pFD::GFP:FD fd-2*), blue dots indicate gene expression in *fd-2*. Mean expression in control and *fd-2* is indicated by red and blue lines, respectively.

A

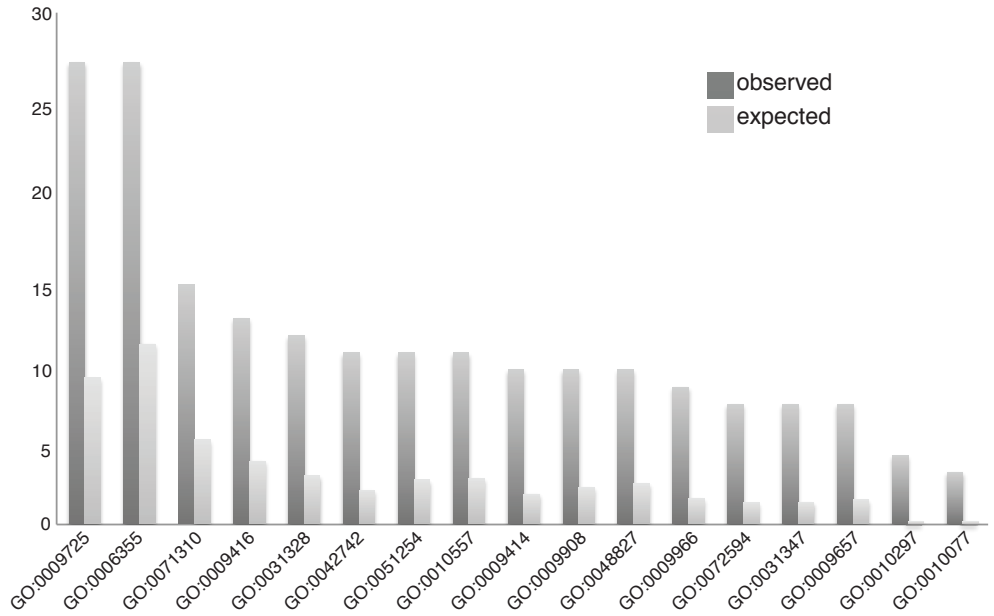

GO:0009725 response to hormone	GO:0009908 flower development
GO:0006355 regulation of transcription, DNA-templated	GO:0048827 phyllome development
GO:0071310 cellular response to organic substance	GO:0009966 regulation of signal transduction
GO:0009416 response to light stimulus	GO:0072594 establishment of protein localization to organelle
GO:0031328 positive regulation of cellular biosynthetic process	GO:0031347 regulation of defense response
GO:0042742 defense response to bacterium	GO:0009657 plastid organization
GO:0051254 positive regulation of RNA metabolic process	GO:0010207 photosystem II assembly
GO:0010557 positive regulation of macromolecule biosynthetic process	GO:0010077 maintenance of inflorescence meristem identity
GO:0009414 response to water deprivation	

B

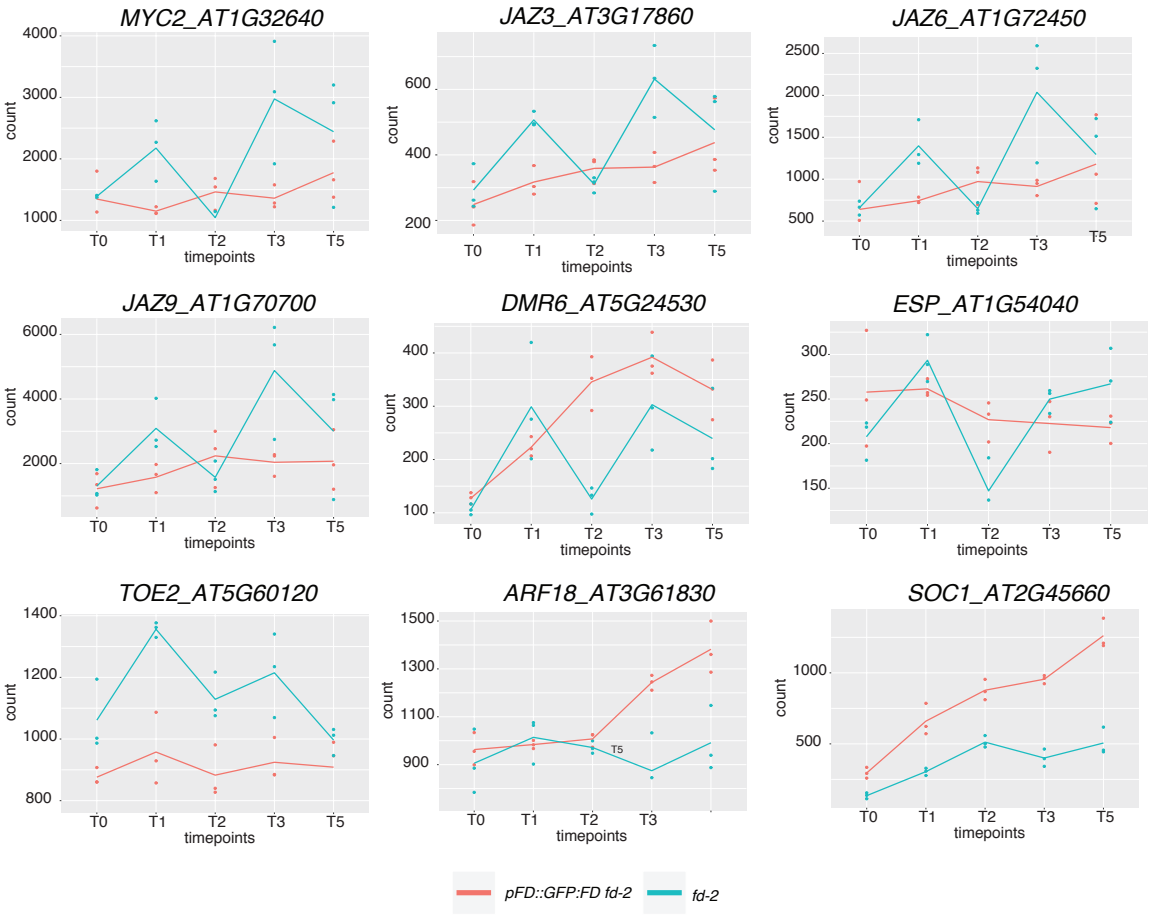

Figure S7. Gene Ontology (GO) analysis on the subset of 135 direct genes of FD.

(A) Significantly enriched GO categories (FDR < 0.05).

(B) Genes with the peculiar expression profile related to pathogen resistance and jasmonate pathway and *ARF18*, gene related to auxin, which share the expression profile with *SOC1*, gene related to gibberellin signaling and important flowering-related gene.

Table S1. List of mutants and oligos for genotyping used in the study.

line	locus	SALK	oligos for screening the mutant		
fd-2	AT4G35900	SALK_013288	WT	Forward	GAAAATAGAAAGTGAGATAAAACC
				Reverse	TGGAAAAGAGAACAGAAGTGAACC
			mut	Forward	ATTTTGCCGATTTCGGAAC
				Reverse	TTCCAAACTTCTTCCATGGTG
ft-10	AT1G65480	GABI_290E08	WT	Forward	ATATTGATGAATCTCTGTTGTGG
				Reverse	AGGGTTGCTAGGACTTGGAACA
			mut	Forward	CCCATTTGGACGTGAATGTAGACAC
				Reverse	AGGGTTGCTAGGACTTGGAACA
tsf-1	AT4G20370	SALK_087522	WT	Forward	CGGTTAACTTGATTTTGTTTCG
				Reverse	ACGTGGACTCTCGTAGCACAC
			mut	Forward	ATTTTGCCGATTTCGGAAC
				Reverse	ACGTGGACTCTCGTAGCACAC
myc2	AT1G32640	SALK_017005C	WT	Forward	CCTACGCTATATTCTGGCAACC
				Reverse	AGTGGCTCTTCTCTACCGTTTG
			mut	Forward	ATTTTGCCGATTTCGGAAC
				Reverse	AGTGGCTCTTCTCTACCGTTTG
afr1	AT1G75060	SALK_026979C	WT	Forward	TTGGCTTAAGAATCACTCCATG
				Reverse	AAAGCGAAGTTGATCTTTGCTC
			mut	Forward	ATTTTGCCGATTTCGGAAC
				Reverse	AAAGCGAAGTTGATCTTTGCTC

Table S2. List of of vectors used in the study.

Construct	Description	Resistance
pLY-33	*pGREEN - pSUC2::GFP:FD*	Spectinomycin
pLY-100	*pGREEN - pSUC2::GFP:NLS*	Spectinomycin
pLY-46	*pGREEN - pFD::GFP:FD*	Spectinomycin
pJM-54	*pGREEN - pFD::FD*	Spectinomycin
pMH-52	*pGREEN - pFD::FD-T282A*	Spectinomycin
pMH-54	*pGREEN - pFD::FD-T282E*	Spectinomycin
pMH-60	*pGREEN - pFD::FD-S281E*	Spectinomycin
pMH-58	*pGREEN - pFD::FD-S281E/T282E*	Spectinomycin
pSC-215	*pGREEN - pFD::C-FD*	Spectinomycin
pSC-216	*pGREEN - pFD::C-FD-T282A*	Spectinomycin
pSC-217	*pGREEN - pFD::C-FD-T282E*	Spectinomycin
pSC-098	*pET-M11 - 6X-His-FD*	Kanamycin
pSC-099	*pET-M11 - 6X-His-FD-T282E*	Kanamycin
pSC-100	*pET-M11 - 6X-His-14-3-3(Nu)*	Kanamycin
pSC-101	*pET-M11 - 6X-His-C-FD*	Kanamycin
pSC-102	*pET-M11 - 6X-His-C-FD-T282E*	Kanamycin
pSC-130	*pET-M11 - 6X-His-FT*	Kanamycin
pSC-166	*pET-M11 - 6X-His-TFL1*	Kanamycin

Table S3. List of of oligos used for qRT-PCR in the study.

gene	locus	oligos for qRT-PCR	
FD	AT4G35900	Forward	GCAAGACTCAAGAGACAACAAG
		Reverse	CAAAATGGAGCTGTGGAAGAC
SOC1	AT2G45660	Forward	AAACGAGAAGCTCTCTGAAAAG
		Reverse	AAGAACAAGGTAACCCAATGAAC
AP1	AT1G69120	Forward	CACCAAATCCAGCATCCTTAC
		Reverse	AGTTCGAGATCATTCCTCCTC
AS1	AT2G37630	Forward	AGAGAGCAGAGAACGGTCCAGG
		Reverse	TCGGTGCCCTTCCTCCAACTCT
SEP1	AT5G15800	Forward	ATGATTGGTGTGAGAAGTCATCATATG
		Reverse	GATGTAACCGTTTCCCTGCTGCGCCTG
SEP2	AT3G02310	Forward	ATCAACAGAATATTGCCTATGGACATC
		Reverse	GATGTAGCCGTTTCCTTGTTGGGACTG
SEP3	AT1G24260	Forward	GGGTATCAGATGCCACTCCAGCTGAAC
		Reverse	AACCCAACATGTAATTATTCACACTTG
SEP4	AT2G03710	Forward	GAGAAAGTTGGAGGACAGTGATGC
		Reverse	GCTCATGCCTTGTTGCTGTTGT
FRI-like 4a	AT3G22440	Forward	GGAGGACTCTAGCAATACTGGCCG
		Reverse	AGCTGATCCAACCGTTTCTTGAGG
FRI-like 4b	AT4G14900	Forward	CCAACAATTCTGGCCGATCTGC
		Reverse	CGGGAATCACGGCTGGTTTTCT
MYC2	AT1G32640	Forward	CGGTGGGGATGGAGATTGAAGTGA
		Reverse	TCAACGCCGACATCAACCTCGC
AFR1	AT1G75060	Forward	TGCTCTTCCGAATCCCACAAAG
		Reverse	TGCAGCCTGAACGAATCCCACA